PROCEEDINGS OF SCIENCE

CP violation in $B_s^0 \to J/\psi\phi$ decay and P_5' and $K\mu\mu$ angular analysis

Chandiprasad Kar on behalf of the CMS Collaboration[a,b,*]

[a] *National Institute of Science Education and Research, India*

[b] *now at Université Clermont Auvergne, CNRS/IN2P3, LPC, Clermont-Ferrand, France*

E-mail: chandiprasad.kar@cern.ch

In these proceedings, the recent measurements of the CP violating phase ϕ_s in $B_s^0 \to J/\psi\phi$ decay using the data collected by CMS experiment at LHC between the years 2017 and 2018 have been presented. The obtained results are combined with the previous CMS measurements, which is also discussed in this paper. Then the measurements of angular parameters in $B^0 \to K^{*0}\mu^+\mu^-$, $B^+ \to K^+\mu^+\mu^-$, and $B^+ \to K^{*+}\mu^+\mu^-$ decay modes using the data collected by CMS experiment in 2012 are presented.

BEAUTY2023
3-7 July 2023
Clermont-Ferrand, France

*Speaker

PoS(BEAUTY2023)006

1. Introduction to CP violation

The CP-violating phase ϕ_s emerges as a result of interference between the B_s^0 meson decay both directly and indirectly via B_s^0 - $\bar{B}_s^0$ mixing to a CP eigenstate. In the absence of BSM (beyond-standard-model) physics in the B_s^0 mixing and decays, a value of $-2\beta_s$ of $-36.96^{+0.72}_{-0.84}$ mrad is determined [1]. However, the presence of BSM particles in B_s^0 mixing has the potential to alter this phase. Given the high precision with which we know the value of ϕ_s in the SM, any variation from this number would be indicative of BSM physics [2]. On the other hand, the decay width difference between the B_s^L and B_s^H eigenstates is predicted with less precision at $\Delta\Gamma_s = 0.082 \pm 0.005$ ps^{-1} [3]. The ability to measure it is crucial for verifying theoretical predictions and putting additional limits on novel physics effects.

1.1 Methodology

The phase ϕ_s is measured by using the data from proton-proton (pp) collisions that were recorded in 2017-2018 by the CMS experiment [4] at $\sqrt{s} = 13$ TeV [5], which amounts to an integrated luminosity of 96.4 fb^{-1}. The $B_s^0 \to J/\psi\phi$ decay channel is studied reconstructing the J/ψ in the $\mu^+\mu^-$ decay channel and the ϕ in the K^+K^- decay channel. To get a maximum signal purity, a dedicated selection on the kinematic variables and on the proper decay time of the B_s^0 decay products is applied.

Using a dedicated tagging trigger requiring three muons in the event (two for J/ψ reconstruction and one for flavour tagging), and a state-of-the-art opposite-side muon flavour tagger based on Deep Neural Networks the analysis sensitivity to ϕ_s improves. Together, these improvements raise the efficiency of muon tagging by a factor of about 10, and result in an overall performance boost of about 20% relative to that reported in Ref. [6].

The weak phase ϕ_s and $\Delta\Gamma_s$ along with several other physics parameters are measured by performing an unbinned multidimensional extended maximum-likelihood fit on the combined data samples using the B_s^0 mass, the B_s^0 proper decay time ct and its uncertainty σ_{ct}, the decay angles of the decay products $(\theta_T, \psi_T, \phi_T)$, the flavour of the B_s^0 at production time, and the mistag ratio w_{tag}, which accounts for the level of reliability of the flavour information.

This analysis accounts for potential contributions from both $B_s^0 \to J/\psi f_0(980)$ and non-resonant $B_s^0 \to J/\psi K^+K^-$ decays by incorporating an additional S-wave amplitude term into the decay model. The fitting model also encompasses background characterization, comprising two terms to describe both the combinatorial background and the peaking background, primarily originating from $B^0 \to J/\psi K^* \to \mu^+\mu^-K^+\pi^-$. To account for efficiency variations, efficiency functions are included to capture the dependence of the signal reconstruction efficiency on the proper decay time and the three angles in the transversity basis. The resulting count of signal events for $B_s^0 \to J/\psi\phi$ from the fit is $48,500 \pm 250$.

1.2 Results

The CPV phase is measured to be $\phi_s = -11 \pm 50\,(\text{stat}) \pm 10\,(\text{syst})$ mrad, while the decay width difference is measured $\Delta\Gamma_s = 0.114 \pm 0.014\,(\text{stat}) \pm 0.007\,(\text{syst})$ ps^{-1}. The statistical component dominates the uncertainty in all these observed values. The results are in agreement with the earlier CMS result [6] and therefore combined. The two sets of results are combined

using their respective correlation matrices, with their respective systematic uncertainties treated as uncorrelated. The combined results for the CP-violating phase and lifetime difference between the two mass eigenstates are:

$$\phi_s = -21 \pm 45 \text{ mrad},$$
$$\Delta\Gamma_s = 0.1073 \pm 0.0097 \text{ ps}^{-1}.$$

Figure 1 displays the two-dimensional ϕ_s vs. $\Delta\Gamma_s$ likelihood contours at 68% confidence level (CL) for the individual and combined results, as well as the SM prediction. The results are consistent with one another and with the SM predictions.

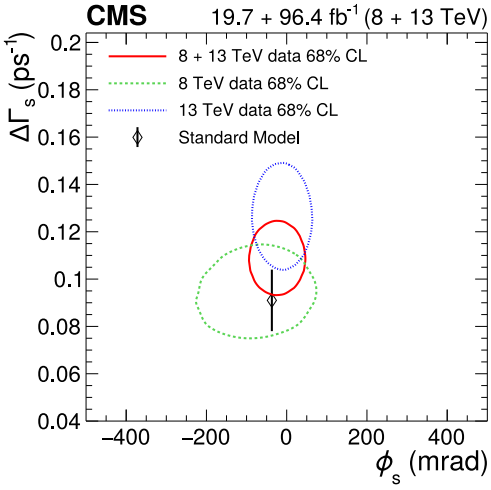

Figure 1: The two-dimensional likelihood contours at 68% CL in the ϕ_s-$\Delta\Gamma_s$ plane, for the CMS 8 TeV (dashed line), 13 TeV (dotted line), and combined (solid line) results. The SM prediction is shown with the diamond marker. More details in Ref. [5].

2. Angular analysis in $b \to s\mu\mu$ decay

The absence of signatures from direct methods has piqued interest in the search for novel physics via indirect approaches. The decay process involving $b \to s\mu\mu$ is particularly promising due to its transition through higher-order box and penguin diagrams, making it highly sensitive to the potential presence of BSM particles within the loop.

The CMS experiment has analysed three decay modes: $B^0 \to K^{*0}\mu^+\mu^-$ where K^* indicates the $K^{*0}(892)$ meson, $B^+ \to K^+\mu^+\mu^-$ and $B^+ \to K^{*+}\mu^+\mu^-$ where K^{*+} indicates $K^{*+}(892)$. The above analyses are based on the pp collision data collected by CMS experiment at centre-of-mass energy 8 TeV. The data corresponds to an integrated luminosity of 20 fb^{-1}.

2.1 Angular analysis of the decay $B^0 \to K^{*0}\mu^+\mu^-$

A comprehensive investigation of the properties of this decay can be achieved by conducting an angular analysis with respect to the dimuon invariant mass squared (q^2). The differential decay

rate for the process $B^0 \to K^{*0}\mu^+\mu^-$ can be expressed using the variables q^2, the decay angle of the dimuon system, θ_l, the decay angle of the K^{*0}, θ_K, and the angle,ϕ , between these two decay planes.

There are a number of angular parameters used to define the angular decay rate; LHCb and Belle observations [7, 8] have drawn attention to the P_5' parameter since they observed a possible tension with the SM. In an effort to shed light on the ambiguity, CMS performed a measurement of the angular parameters P_1 and P_5' [9].

The measurements are carried out over the range of q^2 from 1 to 19 GeV^2 and are then categorised into 9 different bins. Bins $8.68 < q^2 < 10.09$ GeV^2 and $12.90 < q^2 < 14.18$ GeV^2 are utilised as control channels to validate the study because they contain the $B^0 \to K^{*0}J/\psi$ and $B^0 \to K^{*0}\psi(2S)$ decays which has identical final state as of the non-resonant decays of interest. The angular parameters are extracted from the fit to B invariant mass and angular variables. The results are shown in Figure 2.

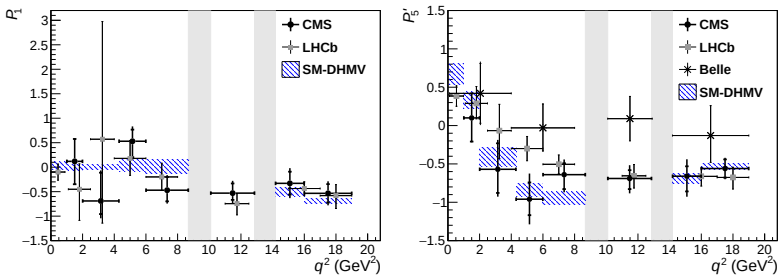

Figure 2: The measured P_1 and P_5' parameters versus q^2 for $B^0 \to K^{*0}\mu^+\mu^-$ decays are shown, in comparison to results from the LHCb and Belle Collaborations. Inner vertical bars reflect statistical uncertainties, whereas outer vertical bars show total uncertainties. SM predictions averaged over q^2 bins are shown in the hatched region. Details can be found in Ref. [10]

2.1.1 Projections for P_5' measurement at the High-Luminosity LHC

The precision of the P_5' parameter measurement from the $B^0 \to K^{*0}\mu^+\mu^-$ analysis has been extrapolated to the expected data-taking conditions and integrated luminosity of HL-LHC [10]. The study of data at 8 TeV [9] serves as a starting point for the extrapolation. The effect of the CMS Phase-II upgrade on the efficiency and mass resolution of the B^0 candidate reconstruction is assessed using simulated events. The predicted increase in mass resolution as a function of q^2 is depicted on Figure 3. The uncertainties of the P_5' results of the 8 TeV study are scaled using the calculated signal yield from the HL-LHC data-taking. The increase in signal yield lead to proportional increases in the statistical and some of the systematic uncertainties. Assuming a general improvement in the analysis procedures, this equates to a factor of two reduction in the other systematic uncertainties. Figure 3 displays the resulting uncertainty with the same central values as the 8 TeV analysis. The total uncertainty is expected to improve by factor 15 with respect to the Run1 results.

2.2 Angular analysis of the decay $B^+ \to K^+\mu^+\mu^-$

The angular decay rate of this decay depends on one angular variable, θ_l, where θ_l is the angle between the direction of μ^- and K^+ in the dileptonic rest frame. Similar to the above mentioned

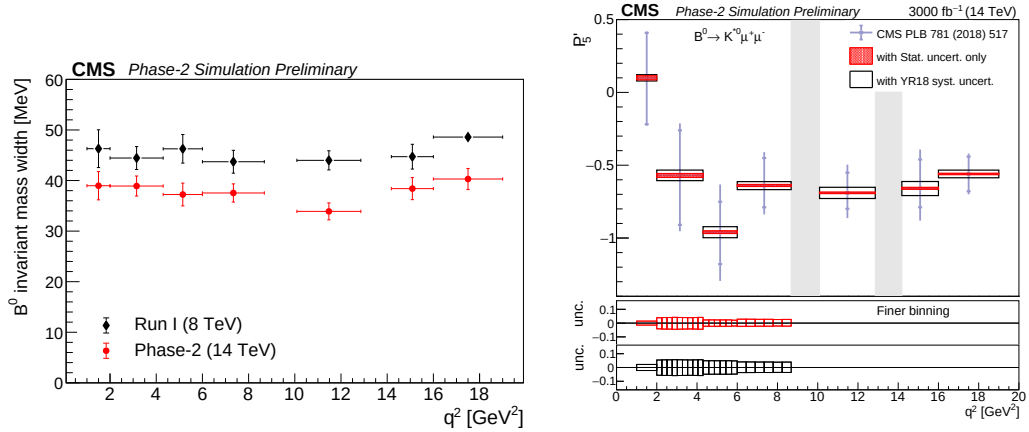

Figure 3: The plot on the left illustrates the relationship between the projected mass resolution and q^2, while the plot on the right presents the projected statistical uncertainties (depicted by hatched regions) and the overall uncertainties (represented by open boxes) for the parameter P_5' as functions of q^2 under the Phase-2 scenario, considering an integrated luminosity of 3000 fb^{-1}. For the more precise q^2 binning, the upper and lower pads stand for the statistical and total uncertainty, respectively. Details can be found in Ref. [9].

analysis the q^2 are divided in to different bins and the resonant bins are used for the validation study. Two independent parameters the muon forward-backward asymmetry, $A_{\rm FB}$ and the $F_{\rm H}$ are extracted from the two dimensional unbinned maximum likelihood fit to the invariant mass of $K^+\mu^+\mu^-$ and cos θ_l.

The measured value of $A_{\rm FB}$ and $F_{\rm H}$ as a function of q^2 are shown in Figure 4[11].

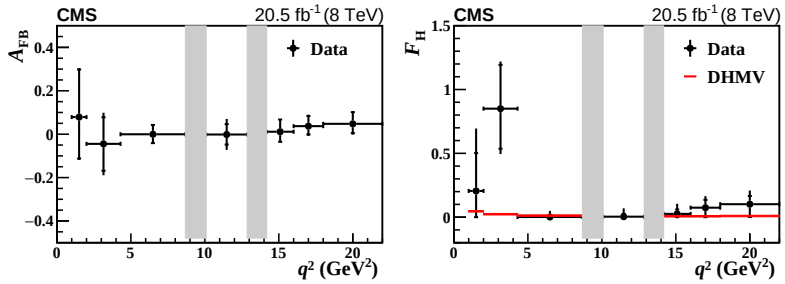

Figure 4: Results of the $A_{\rm FB}$ (left) and $F_{\rm H}$ (right) measurements in ranges of q^2. The statistical uncertainties are shown by the inner vertical bars, while the outer vertical bars give the total uncertainties. The red horizontal lines in the right plot show the DHMV SM theoretical predictions [11].

2.3 Angular analysis of the decay $B^+ \to K^{*+}\mu^+\mu^-$

In the analysis of the $B^+ \to K^{*+}\mu^+\mu^-$ decay, the offline reconstruction requires two oppositely charged muons and a K^{*+} meson. The K^{*+} meson is reconstructed via its decay into the $K_s^0\pi^+$ mode, while the identification of the K_s^0 meson is achieved through its decay into $\pi^+\pi^-$. To describe the theoretical decay rate, along with q^2 three angles are required. The analysis is performed in the bins of q^2 to extract the two decay observables $A_{\rm FB}$ and the K^{*+} longitudinal polarization fraction, F_L.

Since the extracted angular observables $A_{\rm FB}$ and F_L do not depend on ϕ, this angle is integrated out. The parameters of interest are extracted from the three dimensional fit to $K^{*+}\mu^+\mu^-$ invariant mass and two angular variables. The q^2 bin is divided into three bins and two resonant bins for validation of method. The results obtained from the fit are shown in Figure 5 [12]. The uncertainties are dominated by the statistical errors. The results are consistent with the SM predictions.

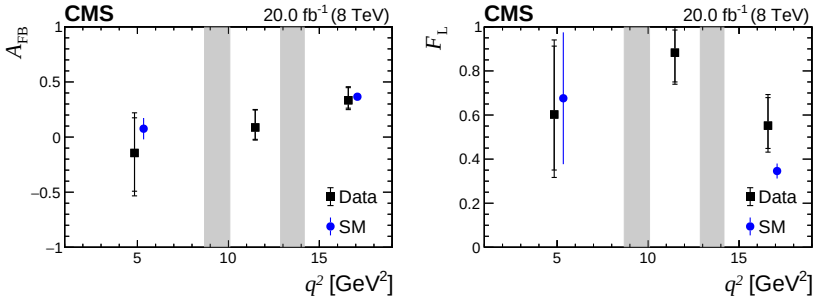

Figure 5: The measured value of $A_{\rm FB}$ (left) and F_L (right) versus q^2 for $B^+ \to K^{*+}\mu^+\mu^-$ decay. The SM predictions and associated uncertainties are shown in filled circle and vertical bars [12].

3. Summary

In summary, a measurement of the weak phase ϕ_s and $\Delta\Gamma_s$ have been presented based on the pp collision data collected by the CMS experiment at the LHC during 2017-2018. The measured values are in agreement with the SM prediction and with the earlier CMS measurement at $\sqrt{s}$ = 8 TeV.

In addition, three angular analyses in the $b \to s\mu\mu$ process have been discussed as well. It is noteworthy that all these measurements are predominantly influenced by statistical uncertainties. Ongoing efforts are focused on improving these measurements with Run-2 data, which may provide insights into the possible presence of BSM physics.

Furthermore, the study reports the projection of the P_5' parameter in the $B^0 \to K^{*0}\mu^+\mu^-$ analysis, utilizing an anticipated dataset of 3000 fb^{-1}, assuming all expected detector-related improvements.

References

[1] The CKM fitter Group Collaboration, Phys. Rev. D 84 (2011) 033005.

[2] C. W. Chiang et al., JHEP 04 (2010), 031 doi:10.1007/JHEP04(2010)031

[3] Particle Data Group (PDG), Prog. Theor. Exp. Phys. 2022, 083C01 (2022) doi:10.1093/ptep/ptac097

[4] CMS Collaboration, JINST 3 (2008) S08004, doi:10.1088/1748-0221/3/08/S08004

[5] CMS Collaboration, Phys. Lett. B 816 (2021) 136188

[6] CMS Collaboration, Phys. Lett. B 757 (2016), 97-120

[7] LHCb Collaboration, JHEP 1602 (2016) 104

[8] Belle Collaboration, Phys. Rev. Lett. 118 (2017) no.11, 111801

[9] CMS Collaboration, Phys. Lett. B 781 (2018) 517

[10] CMS Collaboration, CMS-PAS-FTR-18-033, https://cds.cern.ch/record/2651298

[11] CMS Collaboration, Phys. Rev. D 98 (2018) 112011

[12] CMS Collaboration, JHEP 04 (2021) 124